Earthline Journal of Mathematical Sciences
E-ISSN: 2581-8147
Volume 16, Number 2, March 2026, Pages 269-292
https://doi.org/10.34198/ejms.16226.21.269292

Mixed Convective EMHD Flow in Stratified Fluids over a Stretching Plate with Single Slip and Cross-Diffusion

Golbert Aloliga[1,*], Enoch Deyaka Mwini[2], Isaac Azure[3] and Christian John Etwire[4]

[1] St. Vincent College of Education, P.O Box YD 184 Yendi, Northern Region, Ghana
e-mail: aloligagolbert@gmail.com

[2] Department of Mathematics/ICT, Tamale College of Education, Tamale, Ghana
e-mail: nokyman77@gmail.com

[3] Department of Mathematics, Kwame Nkrumah University of Science and Technology-Kumasi, Ghana
e-mail: isaac.azure@knust.edu.gh

[4] C. K. Tedam University of Technology and Applied Sciences, P. O. Box 24, Navrongo, Ghana
e-mail: jecpapa@yahoo.com

Abstract

This study examines the influence of stratification on mixed convective electro-magnetohydrodynamic (EMHD) flow over a stretching plate in the presence of velocity slip conditions. The analysis is motivated by the relevance of EMHD flows in advanced thermal management systems, microfluidic devices, and electrically conducting fluids subjected to magnetic fields. The coupled governing equations describing momentum, heat transfer, and mass diffusion within the boundary layer are formulated as nonlinear partial differential equations. By introducing appropriate similarity transformations, these equations are reduced to a system of ordinary differential equations, enabling efficient numerical treatment.The resulting boundary value problem is solved numerically using a shooting technique based on Newton's–Raphson method in conjunction with a fourth-order Runge–Kutta integration scheme. The effects of key physical parameters, including magnetic field strength, Biot number, chemical reaction parameter, Eckert number, Prandtl number, Lewis number, suction parameter, and thermal stratification, are systematically investigated. The numerical results reveal that an increase in magnetic field intensity, Biot number, chemical reaction rate, Eckert number, and thermal stratification parameter leads to a significant enhancement in thermal boundary layer thickness, indicating stronger thermal diffusion within the flow field. In contrast, higher values of the Prandtl number, suction parameter, and Lewis number are found to suppress thermal boundary layer development due to reduced thermal and mass diffusivity.

Overall, the findings provide valuable insights into the complex interplay between electromagnetic effects, stratification, and transport phenomena in EMHD flows, contributing to the improved design and optimization of engineering systems involving stratified electrically conducting fluids.

Received: January 8, 2026; Revised & Accepted: February 11, 2026; Published: February 18, 2026
2020 Mathematics Subject Classification: 76W05.
Keywords and phrases: stratification, slips, magnetic field, electro-magnetohydrodynamic, cross-diffusion.
*Corresponding author

Nomenclature

(x, y)	Cartesian coordinates
(u, v)	Velocity components along the x and y axes
B	Solutal stratification coefficients
T_∞	The free-stream temperature of fluid
T_w	Temperature of the sheet
T	Temperature of fluid
c_p	Specific heat at constant pressure
k'	Permeability of the porous media
K	Permeability parameter
D_m	Mean diffusion coefficient
k_t	Thermal-diffusion ratio
c_s	Concentration susceptibility of the fluid
S_o	Soret number
g	Acceleration due to gravity
q_1	Velocity slip parameter
q_2	Temperature slip coefficient
q_3	Concentration slip coefficient
Q_3	Solutal slip parameter
Le	Lewis number
N_B	Buoyancy ratio parameter
q_m	Wall mass flux
h_f	Heat transfer coefficient
Pr	Prandtl number
C_f	Skin-friction coefficient
Re	Reynolds number
Nu	Nusselt number
q_w	Wall heat flux
Br	Brinkman number
U_∞	Free stream velocity of the fluid
S	Suction parameter
C	Concentration of fluid
C_∞	Free-stream concentration of fluid
C_w	Concentration of the sheet
D	Diffusion coefficient
T_m	The mean temperature of the fluid
Sh	Sherwood number
S_s	Solutal stratification parameter
R_i	Richardson number
M	Magnetic field parameter
E	Electric field parameter
Q_1	Momentum slip parameter
Q_2	Thermal slip parameter

Symbols

η	Dimensionless Variable
τ_w	Wall shear stress
ν	Kinematic viscosity of fluid
ρ	Density of fluid
α	Thermal diffusivity of fluid
ρ_∞	Ambient density of the fluid
θ	Dimensionless Temperature
γ	Reaction rate parameter
ϕ	Dimensionless concentration
α_v	Viscoelastic parameter
β	Chemical reaction rate parameter
ρ_p	The density of the fluid particles
ψ	Stream function

1 Introduction

The study of free convective magnetohydrodynamic (MHD) flow in micropolar fluids with double stratification plays a vital role in fluid dynamics, as explored by [1]. Research on

electro-magnetohydrodynamic (EMHD) micropumps under spatially varying magnetic fields suggests that an increase in the magnetic field decay factor results in a reduction in EMHD velocity. In contrast, greater electric field strength enhances velocity, as indicated by [2]. The dynamics of MHD flows impacted by thermal effects and chemical reactions in porous media have been thoroughly studied in recent years. Through a porous medium with a heat source, the impact of chemical processes and Soret effects on MHD free convection flow via an accelerated vertical plate has been examined [3]. Their results demonstrate the importance of thermal diffusion in isotope separation, particularly in gas mixtures that contain light molecules such as helium and hydrogen. The effects of temperature stratification on MHD nanofluid radiative flow over a nonlinear stretching sheet were investigated, observing improvements in temperature, velocity, and nanoparticle concentration [4]. The impact of chemical reactions on MHD-Casson nanofluid flow over a porous stretching sheet with suction and injection was investigated in [5], thereby advancing understanding. Their work advances our knowledge of how chemical processes and magnetic fields affect non-Newtonian fluids. Similarly, [6]found that in thermally mixed convective stratified MHD nanofluid flow with viscous dissipation, higher thermal stratification parameters lead to reduced temperature and concentration profiles. Additionally, [7] investigated radiative MHD Walter's Liquid-B flow past a semi-infinite vertical plate with a heat source and viscous dissipation. Their research highlights how radiation and viscous dissipation interact to affect non-Newtonian fluid movements. The intricate relationships in such systems were further highlighted by [8] investigation of chemical reactions and Hall effects on unsteady flow past an isothermal vertical plate in a rotating fluid with variable mass diffusion and heat source. An analytical solution for transient free-convection MHD flow through a porous medium between two vertical plates with a heat source was presented in another paper by [9], which provided important analytical insights into such arrangements. The effects of heat generation and hall current on free convection flow on a vertical plate were greatly influenced by [10]. When the induced magnetic field was ignored, the magnetic Reynolds number was observed to be low. [11] examined the influence of double stratification on mass and heat transfer in non-uniform MHD nanofluid flow, employing the Runge-Kutta-Fehlberg fourth-order algorithm. Their findings revealed that while thermal stratification reduces fluid temperature, solutal stratification lowers nanoparticle concentration.

Non-Fourier energy transport in double-stratified nanofluid flow past a permeable shrinking/stretching surface was explored [12], noting that solutal and thermal stratification parameters slightly increased temperature and concentration. In [13] an investigation was conducted on the effects of Dufour and Soret numbers on unstable MHD mass and heat transport, considering thermophoresis and non-uniform heat generation. Their results indicated that raising the Soret number or decreasing the Dufour number lowered skin friction and heat transport for shrinking sheets, while the opposite was true for stretching sheets.

Other significant contributions include the work of [14] who analyzed Ohmic heating in Casson fluid MHD mixed convection flow, and [15] who examined Dufour and Soret effects on mass and heat transfer, identifying a wave-like pattern along the y-axis. Additionally, [16] applied the Homotopy analysis method to assess these effects in MHD natural convection of fluid under thermal stratification while [17] explored how the Soret and Dufour numbers impact binary chemical reactions and thermal radiation in

Darcy-Forchheimer nanofluid flow, emphasizing their role in temperature and concentration enhancement.

Other researchers, such as [18], investigated forced convection flow using Buongiorno's nanofluid theory around a moving needle, determining that increased needle thickness reduces mass and heat transfer rates, MHD mixed convection nanofluid flow over nonlinear surfaces was assessed by [19], concluding that stronger Soret effects raise Soret number values, while higher magnetic fields diminish velocity distribution.

Further studies, including those by [20] on mass and heat transfer in MHD slip flow of viscoelastic fluids. [21] demonstrated that chemical reactions in unsteady Maxwell fluid flow suppress velocity fields, while [22] identified key factors affecting heat transfer processes in permeable plate stretching. Elsewhere, [23] studied boundary layer flow in mixed convection over a vertical slender cylinder, and [24] examined viscoelastic fluid flow with variable thermal conductivity, finding that boundary layer thickness changes with temperature and velocity variations. [25] explored ferromagnetic fluid behavior, revealing that temperature rises with velocity slip and ferromagnetic parameters but decreases with buoyancy and Prandtl numbers. The applications of magnetohydrodynamic (MHD) fluxes through porous media in a variety of disciplines, such as environmental science, physics, and engineering, have attracted a lot of interest. The impact of convective boundary conditions, chemical processes, and radiation absorption on MHD flows has been investigated recently. The effects of chemical reactions and radiation absorption on MHD flow through a porous medium past an exponentially accelerated inclined plate with varying temperatures were examined by Balreddy et al. [24]. The importance of chemical reactions and radiation absorption on the flow characteristics was brought to light by their studies. The Keller Box technique explored by [26] was used to analyze heat sink effects on MHD Casson nanofluid stagnation flow, noting a reduction in thermal boundary layer thickness with increasing Prandtl number. The effects of radiation absorption and chemical reactions on convective flows over a porous vertical wavy channel with moving thermal waves were investigated by [27]. Their findings illustrated the importance of chemical reactions and radiation absorption on the properties of flow and heat transfer. These investigations show how crucial it is to take convective boundary conditions, chemical processes, and radiation absorption into account when analyzing MHD flows in porous surfaces. The intricate relationships between these variables and how they affect flow and heat transfer properties require more investigation. [28] studied heat transfer in Maxwell, Jeffery, and Oldroyd-B nanofluids, concluding that stronger heat source or sink parameters elevate thermal boundary layer thickness.

Additional insights were provided by [29] who investigated Maxwell nanofluid stagnation point flow, showing that velocity boundary layer thickness is influenced by the velocity ratio parameter, Maxwell parameter, and magnetic field strength. [30] research focused on Maxwell nanofluid observed reduced velocity but increased temperature profiles in chemically reactive Maxwell nanofluid flow. Hashmi and friends [31] studied buoyancy-driven convection in magnetized Maxwell fluids with homogeneous-heterogeneous reactions, finding that heat transmission varies depending on the stretching parameter and Prandtl number. [32] examined radiative mixed convection in Maxwell nanofluids, discovering that increasing Maxwell parameters enhances stress relaxation, affecting fluid flow properties. Again, [33] emphasized the industrial significance of MHD flow in Maxwell fluids for manufacturing,

and [34] applied spectral relaxation techniques to analyze Maxwell fluid MHD flow, finding that magnetic strength, porosity, Deborah number, and thermal radiation all influence temperature variations. Again [35] explored slip effects on heat transfer in magnetized UCM fluid through porous media, determining that rising thermal relaxation parameters enhance heat transfer rates. Whilst [36] performed a numerical investigation to scrutinize thermal transmission of Carreau nanoliquid, [37] noticed that the new technological fluids with augmented thermal properties gave better results than regular nanofluids. The significance of nanoparticle shapes over the magnetized flow of engine oil-based nanoliquid across a surface of varied thickness under the action of Buongiorno slip effects was investigated by [38]. Also, [39] results revealed that the occurrence of the magnetic field in the unsteady case had a greater role in the enhancement of heat transfer performance as compared with the steady case. Finally, [40] numerically analyzed the consequence of the Buongiorno slip mechanism and radiative heat on gyrotactic microorganisms containing Casson cross nanoliquid flow across a moving wedge.The present investigation applies to a wide range of engineering and industrial processes involving electrically conducting and stratified fluids under electromagnetic control. In particular, the results are relevant to the design and optimization of electromagnetic microfluidic devices, such as EMHD micropumps and lab-on-a-chip systems, where precise regulation of flow, heat, and mass transfer is required. The model is also applicable to advanced thermal management systems, including cooling of electronic components, nuclear reactors, and high-performance heat exchangers, where magnetic and electric fields are used to control convective transport in porous and stratified.

2 Mathematical Formulation

Consider a steady, two-dimensional, incompressible, and laminar mixed convective flow of an electrically conducting, stratified fluid over a stretching surface within a porous medium. The system incorporates the effects of electric field and magnetic systems as well as slip conditions. An external transverse magnetic field and an electric field, both of specified intensities, are applied to the flow. The coordinate system is defined such that the x-axis runs parallel to the stretching sheet, while the y-axis is perpendicular to it. The stretching plate's velocity is assumed to be proportional to its distance from the origin (that is $u_w = bx$). The stretching sheet's temperature and concentration are $T_w = T_0 + A_1 x$ and $C_w = C_0 + B_1 x$ respectively whereas the fluid's ambient concentration and temperature are $C_\infty = C_0 + B_2 x$ and $T_\infty = T_0 + A_2 x$ respectively.

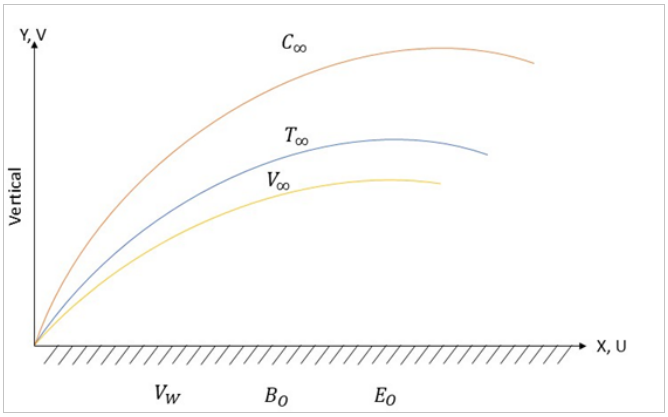

Figure 1: Schematic diagram of the flow.

By the boundary layer approximations, the continuity, momentum, energy and concentration equations modelling the flow problem [41] can be expressed as;

$$\frac{\partial u}{\partial x}+\frac{\partial v}{\partial y}=0 \tag{1}$$

$$u\frac{\partial u}{\partial x}+v\frac{\partial v}{\partial y}=\nu\frac{\partial^2 u}{\partial y^2}-\frac{\sigma B_0}{\rho}(B_0u-E_0)-\frac{v}{k'}u+\frac{1}{\rho}\left[\rho_\infty\beta g(1-C_\infty)(T-T_\infty)-g(\rho_p-\rho_\infty)(C-C_\infty)\right] \tag{2}$$

$$u\frac{\partial T}{\partial x}+v\frac{\partial T}{\partial y}=\alpha\frac{\partial^2 T}{\partial y^2}+\frac{\mu}{\rho C_p}\left(\frac{\partial u}{\partial y}\right)^2+\frac{\sigma}{\rho C_p}(B_0u-E_0)^2+\frac{D_mk_t}{C_sC_p}\frac{\partial^2 C}{\partial y^2} \tag{3}$$

$$u\frac{\partial C}{\partial x}+v\frac{\partial C}{\partial y}=D\frac{\partial^2 C}{\partial y^2}-\gamma(C-C_\infty)+\frac{D_mk_t}{T_m}\frac{\partial^2 T}{\partial y^2} \tag{4}$$

Subject to the boundary conditions [41],

$$u(x,0)=bx,\quad v(x,0)=-v_w,\quad T(x,0)=T_0+A_1x+q_2\frac{\partial T}{\partial y},\quad C(x,0)=C_0+B_1x+q_3\frac{\partial C}{\partial y}\quad \text{at } y=0,$$

$$u(x,\infty)\to 0,\quad T(x,\infty)=T_0+A_2x,\quad C(x,\infty)=C_0+B_2x,\quad \text{as } y\to\infty. \tag{5}$$

3 Similarity Transformations

Equation (1) is satisfied identically by defining the stream function, $\psi(x,y)$, as;

$$u=\frac{\partial\psi}{\partial y}\quad\text{and}\quad v=-\frac{\partial\psi}{\partial x}. \tag{6}$$

The following independent variable η, dimensionless temperature $\theta(\eta)$, stream function, $\psi(x,y)$, and dimensionless concentration $\phi(\eta)$ were used to convert the flow equations into nonlinear ordinary differential equations by substituting (7) into (2), (3), (4), and (5).

$$\eta=y\sqrt{\frac{b}{v}},\quad \psi(x,y)=\sqrt{bv}\,xf(\eta),\quad \theta(\eta)=\frac{T-T_\infty}{T_w-T_0},\quad \phi(\eta)=\frac{C-C_\infty}{C-C_0} \tag{7}$$

$$f'''(\eta) - \left(f''(\eta)\right)^2 + f(\eta)f''(\eta) - Mf'(\eta) + EM + \lambda\left(\theta(\eta) - N\phi(\eta)\right) - Kf'(\eta) = 0 \tag{8}$$

$$\theta''(\eta) + Pr\, f(\eta)\theta'(\eta) + EcM\left(f'(\eta) - E\right)^2 - Pr\,\theta(\eta)f'(\eta) - PrBif'(\eta) + PrN\phi''(\eta) + Ec\left(f''(\eta)\right)^2 = 0 \tag{9}$$

$$\phi''(\eta) + PrLe\, f(\eta)\phi'(\eta) - PrLe\, f'(\eta)\phi(\eta) - PrLeBf'(\eta) - PrLe\beta\phi(\eta) + LePr\,\theta''(\eta) = 0 \tag{10}$$

$$f'(0) = 1, \quad f(0) = S, \quad \theta(0) = (1 - Bi) + Q\theta'(0), \quad \phi(0) = (1 - B) + Q\phi'(\eta)$$

$$f'(\infty) = 0, \quad \theta(\infty) = 0, \quad \phi(\infty) = 0 \tag{11}$$

Where $M = \frac{\sigma B_0^2}{\rho b}$ is the magnetic parameter, $R = \frac{Gr}{Re^2}$ is the Richardson number, $E = \frac{E_0}{B_0 bx}$ is the electric parameter, $K = \frac{\nu}{k'b}$, $G_T = \frac{\beta_T(1-C_\infty)(T_w-T_0)x^2}{\rho v^2}$, $S = \frac{D_m K_t(T_w-T_0)}{vT_m(C_w-C_0)}$, $N = \frac{(\rho_p-\rho_\infty)(C_w-C_0)}{\rho_\infty\beta(C-C_\infty)(T_w-T_0)}$, $Pr = \frac{\nu}{\alpha}$, $Br = \frac{\mu u_w^2 \nu}{(T_w-T_0)}$, $E = \frac{E_0}{B_0 bx}$, $Le = \frac{\alpha}{D}$, $\beta = \frac{\gamma}{b}$.

4 Validation of Model

The outcome of the model for skin friction coefficient represented by $(f''(0))$ was compared with the work of Stanford [34] for different values of Prandtl number and there was excellent agreement with their findings. This validates current model. The comparison is indicated in Table 1.

Table 1: Comparison of values of $f''(0)$ and $-\theta'(0)$ for different values of Pr.

Pr	[34]		Present	
	$f''(0)$	$-\theta'(0)$	$f''(0)$	$-\theta'(0)$
5	0.902783	-0.166676	0.902745	-0.166621
10	0.902624	0.085160	0.902614	0.085131
15	-0.974284	0.085610	-0.974279	0.085658
20	-0.974551	0.085748	-0.974543	0.085742
25	0.902529	0.085778	0.902529	0.085790

5 Impact of Thermophysical Parameters on Coefficient of Skin Friction, Nusselt Number and Sherwood Number

Table 2 shows the impact of thermo-physical parameters on the coefficient of skin friction $(f''(0))$, Nusselt number representing heat transfer rate $(-\theta'(0))$, and Sherwood number representing mass transfer rate $(-\phi'(0))$. An increase in the thermophoretic deposition parameter, momentum slip parameter, and Biot number raise Nusselt number but decrease coefficient of skin friction and Sherwood numbers, as indicated in the table. In addition, raising Solutal Grashof, thermal Grashof, and Damkohler numbers lower skin friction coefficient while raising Nusselt and Sherwood numbers. Raising Eckert number, heat generation parameter Q, and B lower coefficient of skin friction and Nusselt number, while raising the Sherwood

number. Furthermore, increasing the magnetic field parameter and the permeability parameter raise coefficient of skin friction number while lowering Nusselt and Sherwood numbers. Additionally, raising the chemical reaction parameter and Lewis number raise coefficient of skin friction and the Sherwood number, whereas lowering the Nusselt number. Finally, raising the Prandtl number and the suction parameter simultaneously raise skin friction coefficient, Sherwood, and Nusselt numbers.

Table 2: Results of skin friction coefficient $[f''(0)]$, Nusselt $[-\theta'(0)]$ and Sherwood numbers $[-\phi'(0)]$ for various values of controlling parameters.

Pr	Bi	Le	M	N	E	S	K	B	Ec	Q	β	$-f''(0)$	$-\theta'(0)$	$-\phi'(0)$
2	0.1	0.5	0.1	0.1	0.1	0.1	0.1	0.1	0.1	0.1	0.1	0.999023	0.076314	0.087249
3												1.004187	0.079996	0.089901
4												1.006682	0.081745	0.091469
	0.2											0.996334	0.138979	0.087178
	0.3											0.994092	0.191378	0.087117
		0.6										0.000036	0.076299	0.088516
		0.7										1.000777	0.076289	0.089499
			0.2									1.035635	0.075604	0.087133
			0.3									1.070638	0.074909	0.087022
				0.2								0.996530	0.076349	0.087260
				0.3								0.996530	0.076349	0.087260
					0.2							0.992891	0.076387	0.087271
					0.3							0.986812	0.076460	0.087293
						0.2						1.052462	0.078882	0.088169
						0.3						1.052461	0.078882	0.088169
							0.2					1.034247	0.075917	0.087139
							0.3					1.067973	0.075521	0.087033
								0.2				0.997704	0.074148	0.087261
								0.3				0.995994	0.071377	0.087276
									0.2			0.995089	0.068665	0.087289
									0.3			1.001123	0.064611	0.092605
										0.2		0.887843	0.084065	0.092299
										0.3		0.795724	0.084997	0.092103
											0.2	1.008423	0.082750	0.093080
											0.3	1.008636	0.082748	0.093526

5.1 Graphical Result

5.1.1 Variation of parameters on velocity graphs

The impacts of different thermophysical factors on the boundary layer's velocity profiles are shown in Figures 2–7. Increases in magnitudes of suction number and magnetic number result in thicker momentum boundary layer thickness, as seen in Figures 1 and 2. In Figures 4-7, increasing the Eckert parameter, Prandtl number, chemical reaction parameter, heat transfer parameter, and thermal stratification coefficient parameter reduce fluid's velocity, resulting in a thinner momentum boundary layer. Figure 2 shows the velocity graph for the magnetic field number. As the magnetic number increases, there is a sharp decline close to the walls of the plate, and the velocity boundary layer thickness weakens as it agrees with its boundary condition. The velocity of the fluid reduces as the magnetic field parameter increases. Because the magnetic field retards flow, this result qualitatively follows the Lorentz force expectations. Similar effects were shown in Figure 4 for the Prandtl number. Because the Prandtl number is a momentum thermal-diffusivity ratio, it reduces the velocity of the fluid as the Prandtl number rises, as seen in Figure 4. The impact of the chemical reaction parameter in velocity profile is depicted in Figure 5. As the chemical reaction parameter increases, the thickness of the velocity boundary layer reduces, which is due to an increase in viscosity. Figure 7 shows that increasing the thermal stratification coefficient lowers fluid velocity because relaxation time decreases.

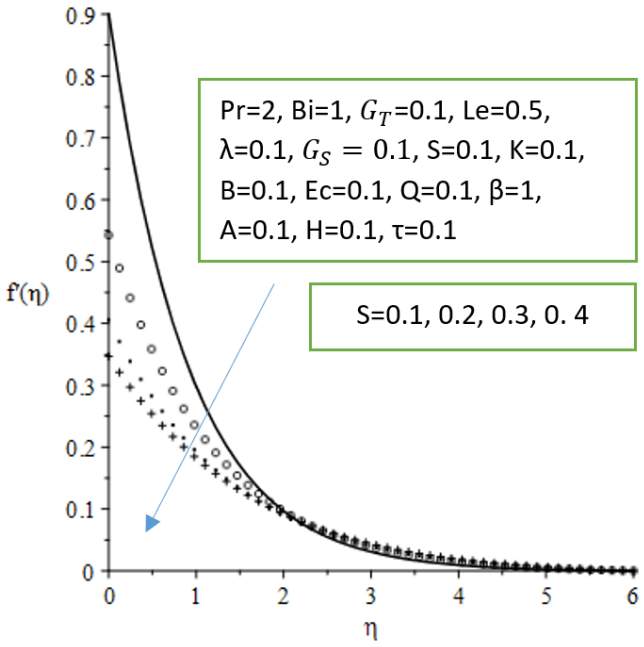

Figure 2: Velocity graph for various values of the suction parameter.

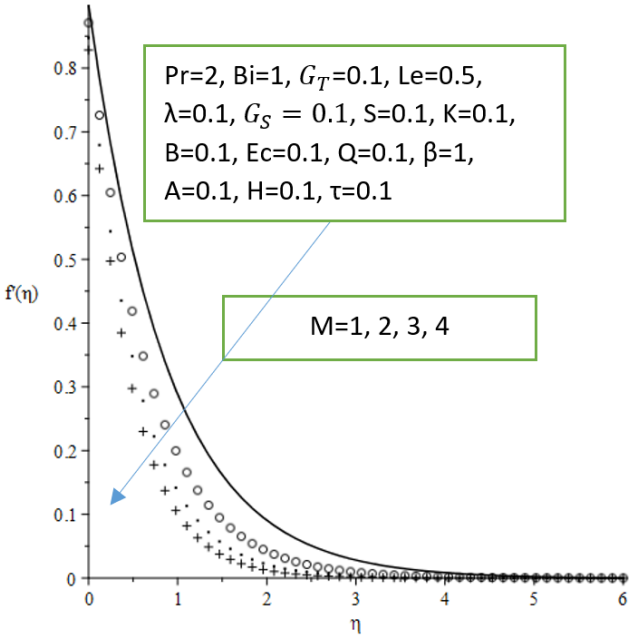

Figure 3: Velocity graph for various values of magnetic field parameter.

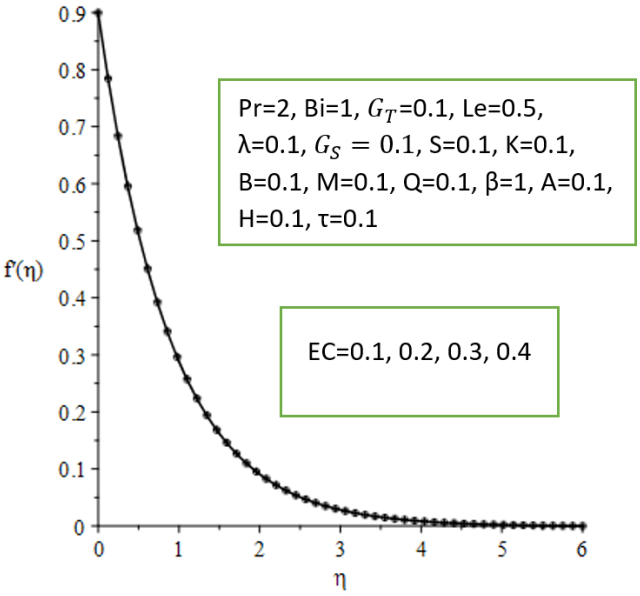

Figure 4: Velocity graph for various values of Eckert parameter.

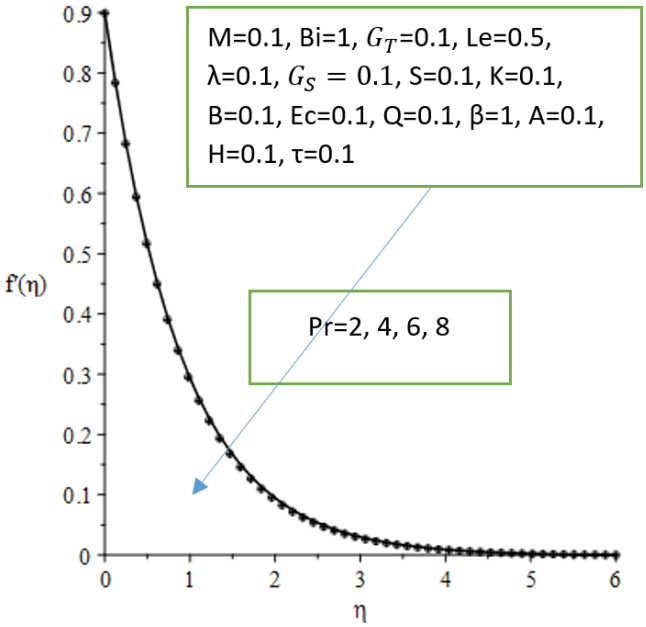

Figure 5: Velocity graph for various values of Prandtl parameter.

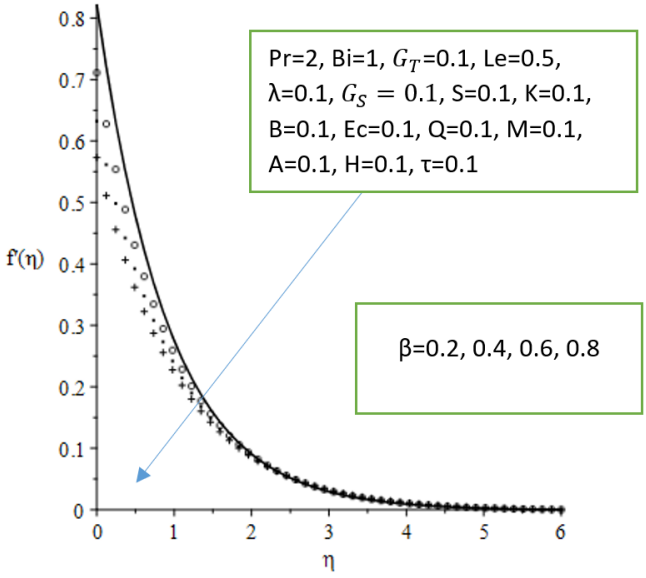

Figure 6: Velocity graph for various values of chemical reaction parameter.

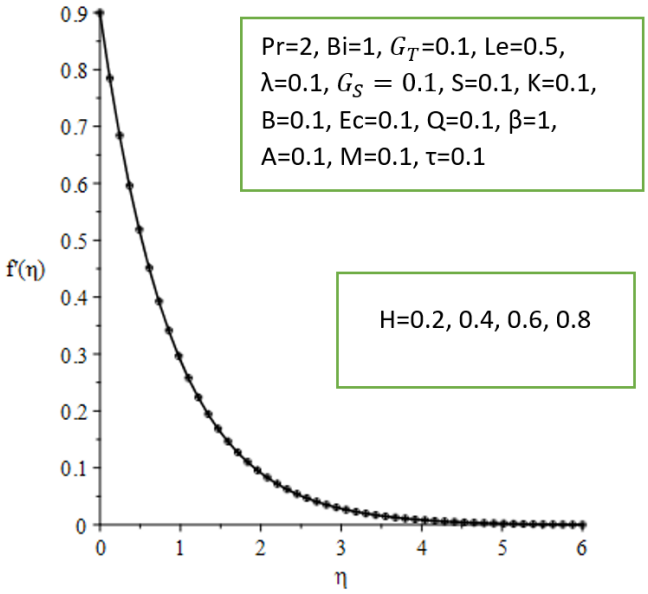

Figure 7: Velocity graph for various values of heat transfer parameter.

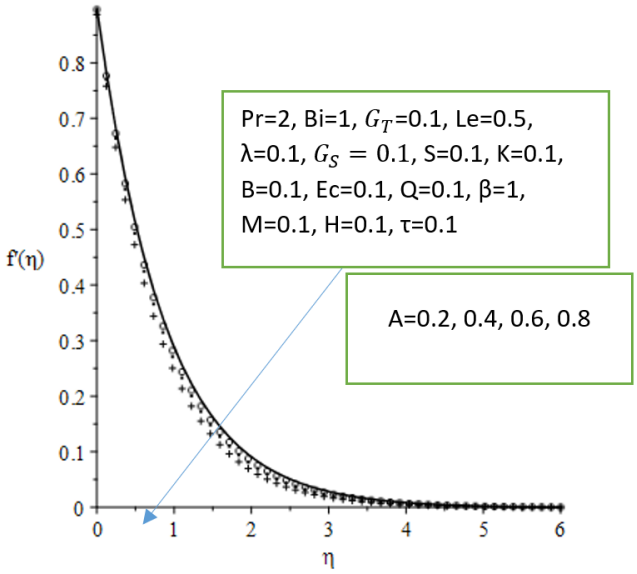

Figure 8: Velocity graph for various values of thermal stratification coefficient parameter.

5.1.2 Variation of parameters on temperature graphs

The effects of various thermophysical parameters on the temperature profiles are presented in Figures 8–12. Generally, increases in the heat generation parameter, chemical reaction parameter, Eckert number, thermal stratification parameter, and magnetic field strength lead to a rise in fluid temperature and

a corresponding thickening of the thermal boundary layer. The Eckert number, in particular, elevates the temperature due to enhanced viscous dissipation, which converts kinetic energy into internal energy, thereby increasing the thermal boundary layer thickness. Similarly, the application of a transverse magnetic field intensifies the temperature profile as a result of the Lorentz force, which resists fluid motion and enhances thermal energy within the boundary layer. Furthermore, higher values of the thermal stratification parameter increase the fluid temperature by amplifying thermal gradients, thus thickening the thermal boundary layer. However, in some cases, increasing the heat transfer coefficient and reaction rate parameter reduces the fluid temperature, leading to a thinner thermal boundary layer due to enhanced heat removal from the surface. Overall, these parameters play a significant role in controlling the thermal behavior of the flow system.

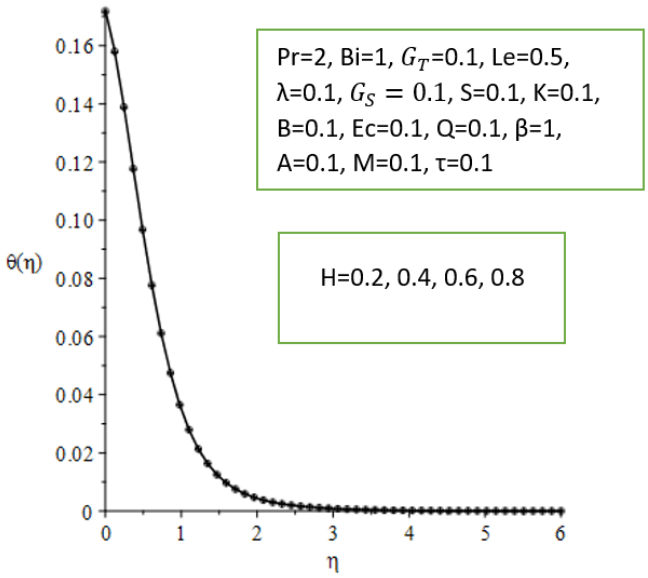

Figure 9: Temperature graph for various values of heat transfer parameter.

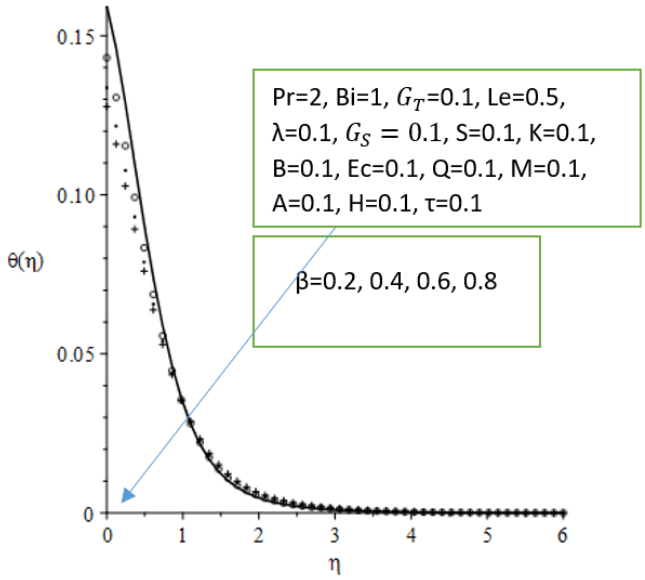

Figure 10: Temperature graph for various values of reaction rate parameter.

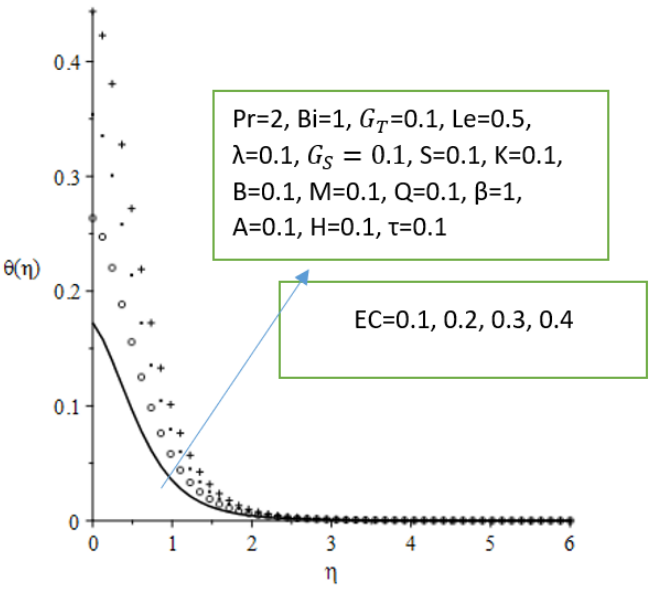

Figure 11: Temperature graph for various values of Eckert parameter.

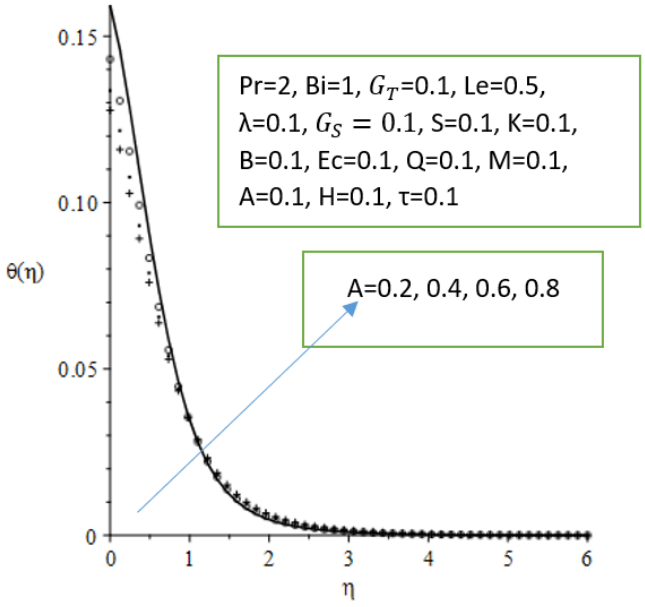

Figure 12: Temperature graph for various values of thermal stratification parameter.

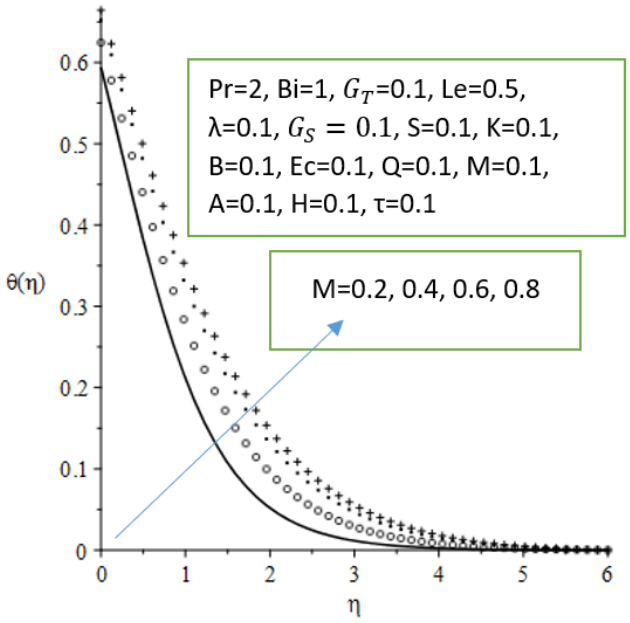

Figure 13: Temperature graph for various values of magnetic field parameter.

5.1.3 Variation of parameters on concentration graphs

The influence of various thermophysical parameters on the concentration profiles is illustrated in Figures 13–20. As shown in Figures 13 and 16, an increase in the magnetic field parameter and the Biot number

leads to higher fluid concentration, thereby thickening the solutal boundary layer. The enhancement in concentration under a stronger magnetic field is attributed to the Lorentz force, which modifies the flow structure and promotes species accumulation near the surface. Conversely, Figures 15, 17, and 19 reveal that increasing the Prandtl number, suction parameter, and Lewis number reduces fluid concentration, resulting in a thinner solutal boundary layer due to enhanced thermal diffusion and mass transport effects. Furthermore, Figure 20 demonstrates that higher values of the permeability parameter increase concentration. This occurs because greater permeability weakens the resistance to fluid motion within the porous medium, reducing mass transport at the surface and intensifying the concentration gradient.

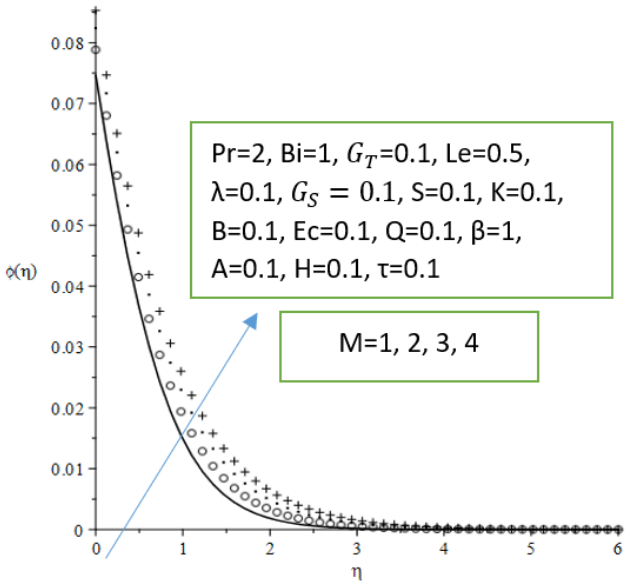

Figure 14: Concentration graph for various values of magnetic field parameter.

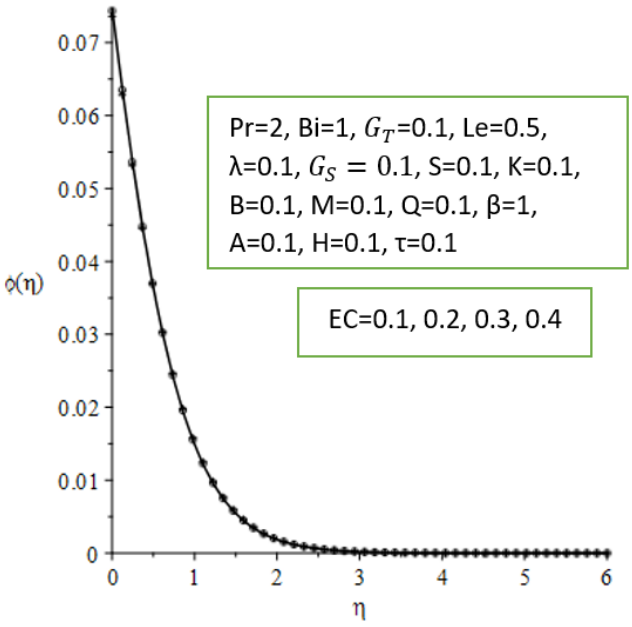

Figure 15: Concentration graph for various values of Eckert parameter.

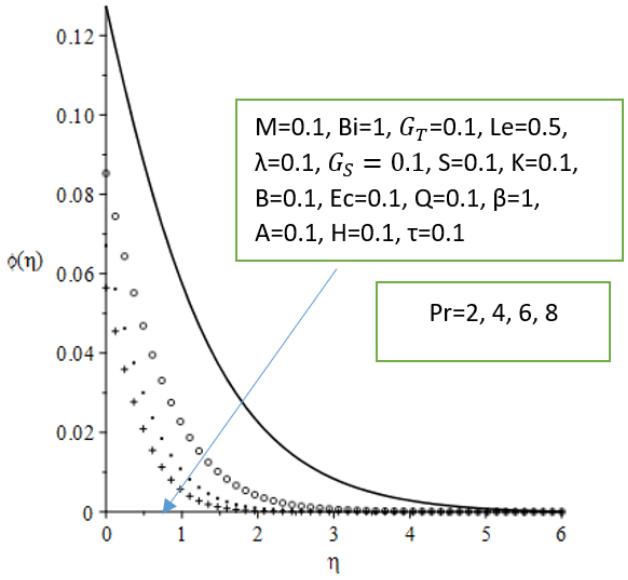

Figure 16: Concentration graph for various values of Prandtl parameter.

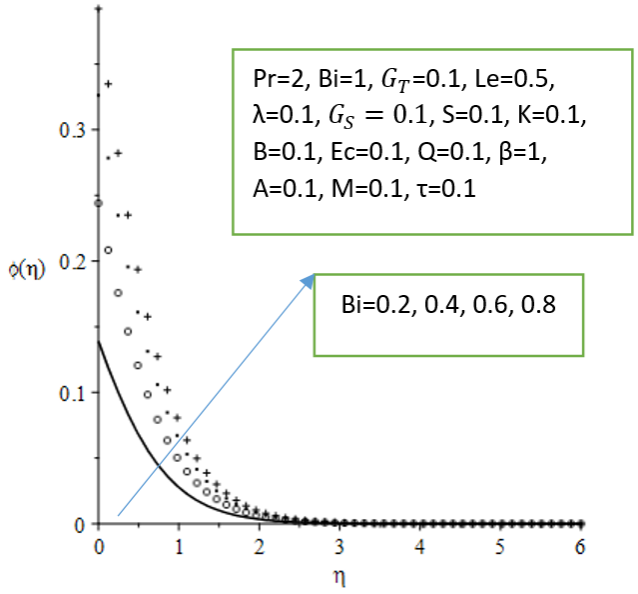

Figure 17: Concentration graph for various values of Biot number parameter.

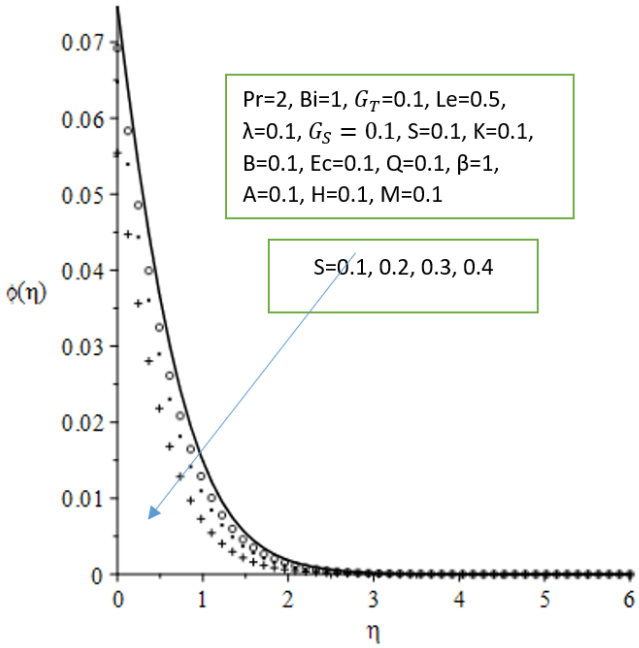

Figure 18: Concentration graph for various values of suction parameter.

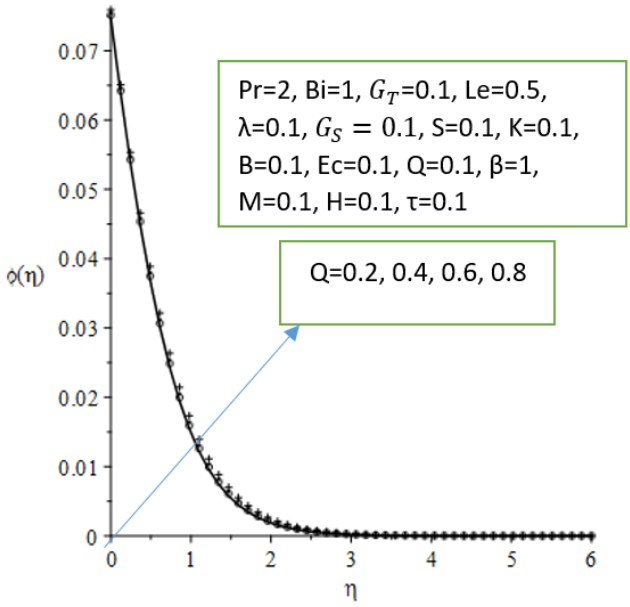

Figure 19: Concentration graph for various values of solutal slip parameter.

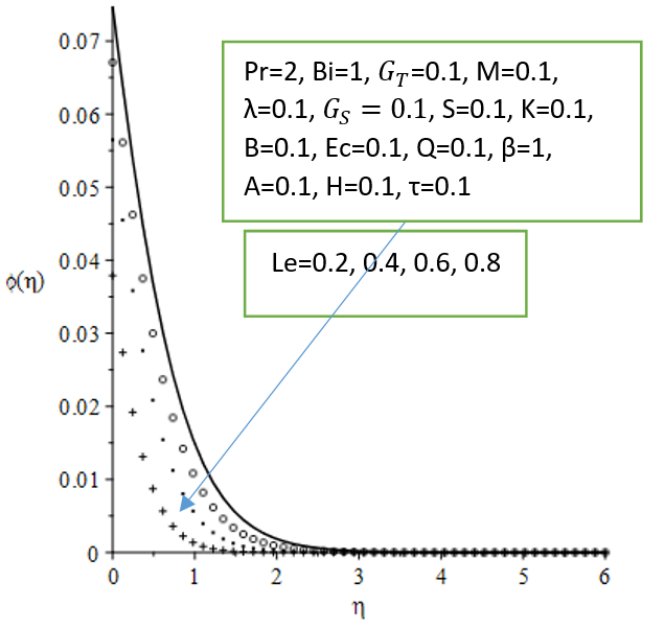

Figure 20: Concentration graph for various values of Lewis parameter.

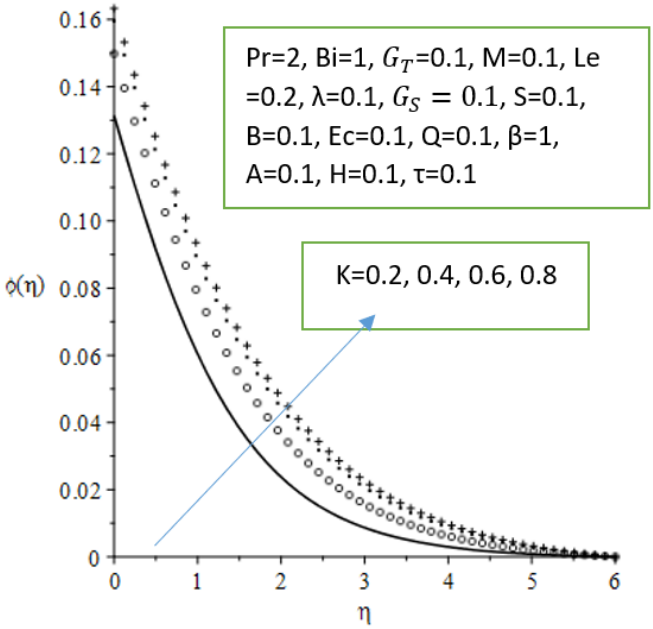

Figure 21: Concentration graph for various values of permeability parameter.

6 Conclusion

This study has demonstrated that the transport characteristics of the mixed convective EMHD flow are strongly influenced by the governing physical parameters. Thermophoretic deposition, momentum slip, and the Biot number were found to enhance heat transfer while simultaneously reducing skin friction and mass transfer rates. In contrast, increasing the Thermal and Solutal Grashof numbers as well as the Damköhler number lowered the skin friction coefficient but significantly improved both heat and mass transfer. Higher values of the Eckert number and heat generation parameter reduced skin friction and heat transfer, although they intensified mass transfer. The Deborah number, magnetic field strength, and permeability parameter increased skin friction but suppressed heat and mass transfer rates. Moreover, larger Lewis number and chemical reaction parameters promoted skin friction and mass transfer while diminishing heat transfer. The momentum boundary layer thickened under the influence of the Damköhler number, heat generation, Grashof numbers, Biot number, and Eckert number, whereas it reduced with increasing Prandtl number, magnetic field, momentum slip, permeability, suction, and Deborah number. The thermal boundary layer expanded with stronger magnetic field, momentum slip, permeability, Biot number, Eckert number, and heat generation effects, while the solutal boundary layer increased with thermophoresis, Damköhler number, magnetic field, slip, and permeability but decreased with higher Prandtl and Lewis numbers, Grashof numbers, Biot number, chemical reaction parameter, heat generation, suction, and Eckert number. Overall, these findings provide comprehensive insight into the control of momentum, heat, and mass transport in EMHD flows relevant to industrial and engineering applications.

7 Conflict of Interest

The authors declared no conflicts of interest for the current study.

8 Funding

The authors did not receive any financial assistance from anywhere for the publication of this paper.

References

[1] Srinivasacharya, D., & Upendar, M. (2013). Effect of double stratification on MHD free convection in a micropolar fluid. *Journal of Egyptian Mathematical Society, 21*, 370–378.

[2] Jian, Y., & Chang, L. (2015). EMHD micropumps under a spatially non-uniform magnetic field. *AIP Advances*, 057121. https://doi.org/10.1063/1.4921085

[3] Chenna, D. K., Seshagiri, R. Y. V., Satheesh, Y. K. R., Vishnuvardhan, V., & Raju, D. (2025). Chemical reaction and Soret effects on MHD free convection flow past an accelerated vertical plate through a porous medium with heat source. *International Journal of Food and Nutritional Sciences, 11*(12), 165–183.

[4] Yahaya, S. D., & Faisal, S. (2018). Impact of thermal radiation on electrical MHD flow of nanofluid over nonlinear stretching sheet with variable thickness. *Alexandria Engineering Journal, 57*, 2187–2197.

[5] Chenna, D. K., Nagaraju, V., & Bhumarapu, V. (2023). Investigating the influence of chemical reaction on MHD-Casson nanofluid flow via a porous stretching sheet with suction/injection. *Science, Engineering and Technology, 3*(2), 47–62.

[6] Besthapy, P., Haq, R. U., Bandari, S., & Al-Mdallal, Q. (2017). Mixed convection flow of thermally stratified MHD nanofluid over an exponentially stretching surface with viscous dissipation effect. *Journal of the Taiwan Institute of Chemical Engineers, 71*, 307–314.

[7] Chenna, D. K., Bhumarapu, V., & Makinde, O. D. (2021). Radiative MHD Walter's liquid-B flow past a semi-infinite vertical plate in the presence of viscous dissipation with a heat source. *Engineering Transactions, 69*(4), 373–401.

[8] Ramesh, B. P., Chenna, D. K., & Seshagiri, R. Y. V. (2024). Chemical reaction and Hall effects on unsteady flow past an isothermal vertical plate in a rotating fluid with variable mass diffusion with heat source. *European Chemical Bulletin, 11*(11), 1432–1446.

[9] Balreddy, G., Chenna, D. K., & Seshagiri, R. Y. V. (2022). Analytical solution for transient free convection MHD flow through a porous medium between two vertical plates with heat source. *European Chemical Bulletin, 11*(10), 653–661.

[10] Balreddy, G., Seshagiri Rao, Y. V., Chenna Kesavaiah, D., & Lavanya, S. (2023). Effects of Hall current and rotation, heat generation on MHD free convection heat and mass transfer flow past an accelerated vertical plate. *Journal of Computational Analysis and Applications, 31*(4), 573–586.

[11] Mutuku, W. N., & Makinde, O. D. (2017). Double stratification effect on heat and mass transfer in unsteady MHD nanofluid flow over a flat surface. *Asia Pacific Journal of Computational Engineering, 4*, 2. https://doi.org/10.1186/S40540-017-0021-2

[12] Khashiie, N. S., Arifin, N. M., & Hafidzuddin, E. H. (2019). Dual stratified nanofluid flow past a permeable shrinking/stretching sheet using non-Fourier energy model. *Applied Sciences, 9*, 2124.

[13] Reddy, P. S., & Chamkha, A. J. (2015). Soret and Dufour effects on unsteady MHD heat and mass transfer from a permeable stretching sheet with thermophoresis and non-uniform heat generation/absorption. *Journal of Applied Fluid Mechanics, 9*(5), 2443–2455. https://doi.org/10.18869/acadpub.jafm.68.236.25171

[14] Gireesha, B., Kumar, K. G., Krishnamurthy, M. R., Manjunatha, S., & Rudraswamy, N. G. (2019). Impact of Ohmic heating on MHD mixed convection flow of Casson fluid by considering cross-diffusion effect. *Journal of Nonlinear Engineering, 8*(1), 380–388. https://doi.org/10.1515/nteng-2017-0144

[15] Gbadeyan, J. A., Oyekunle, T. L., Fasogbon, P. E., & Abubakar, J. U. (2018). Soret and Dufour effects on heat and mass transfer in chemically reacting MHD flow through a wavy channel. *Journal of Taibah University for Science, 12*(5), 631–651.

[16] Oreyeni, T., & Omokhuale, E. (2019). Optimal homotopy analysis of MHD natural convection flow of thixotropic fluid under subjection of thermal stratification: Boundary layer analysis. *American Journal of Computational Mathematics, 9*, 116–131. https://doi.org/10.4236/ajcm.2019.92009

[17] Rasool, G., Shafiq, A., & Baleanu, D. (2020). Consequences of Soret–Dufour effects on thermal radiation and binary chemical reaction on Darcy–Forchheimer flow of nanofluids. *Symmetry, 12*, 1421. https://doi.org/10.3390/sym12091421

[18] Salleh, S. N. A., Bachok, N., Arifin, N. M., & Ali, F. M. (2020). Influence of Soret and Dufour effects on forced convection flow towards a moving thin needle considering Buongiorno's nanofluid model. *Alexandria Engineering Journal, 59*(5), 3897–3906. https://doi.org/10.1016/j.aej.2020.06.045

[19] Jamel, B., Abdelhafez, M. A., Abd-Alla, A. M., Abo-Dahab, S. M., & Mahmot, K. H. (2021). MHD mixed convection nanofluid flow over a convectively heated nonlinear extending surface with Soret effect. *Complexity, 2021*, 5592024. https://doi.org/10.1155/2021/5592024

[20] Turkyilmazoglu, M. (2011). Multiple solutions of heat and mass transfer of MHD slip flow for the viscoelastic fluid over a stretching sheet. *International Journal of Thermal Sciences, 50*(11), 2264–2276. https://doi.org/10.1016/j.ijthermalsci.2011.05.014

[21] Mukhopadhyay, S., & Bhattacharyya, K. (2012). Unsteady flow of a Maxwell fluid over a stretching surface in the presence of chemical reaction. *Journal of the Egyptian Mathematical Society, 20*, 229–239.

[22] Zheng, L., Liu, N., & Zhang, X. (2013). Maxwell fluid unsteady mixed flow and radiation heat transfer over a permeable plate with boundary slip and non-uniform heat source/sink. *Journal of Heat Transfer, 135*(3), 031705. https://doi.org/10.1115/1.4007891

[23] Ellahi, R., Riaz, A., Abbasbandy, S., Hayat, T., & Vafai, K. (2014). Mixed convection boundary layer flow and heat transfer over a vertical slender cylinder. *Thermal Science, 18*, 1247–1258.

[24] Hayat, T., Anwar, M. S., Farooq, M., & Al-Saedi, A. (2015). Mixed convection flow of viscoelastic fluid by a stretching cylinder with heat transfer. *PLoS ONE, 10*(3), Article e0118815. https://doi.org/10.1371/journal.pone.0118815

[25] Zeeshan, A., Majeed, A., Ellahi, R., & Zia, Z. M. (2016). Mixed convection flow and heat transfer in ferromagnetic fluid over a stretching sheet with partial heat flux effect. *Thermal Science, 20*(6), 1783–1794. https://doi.org/10.2298/TSCI160620068Z

[26] Krishnaiah, M., Rajendar, P., Laxmi, T. V., & Reddy, M. C. K. (2017). Influence of non-uniform heat source/sink on stagnation point flow of MHD Casson nanofluid over an exponentially stretching surface. *Global Journal of Pure and Applied Mathematics, 13*(10), 7009–7033.

[27] Venkateswarlu, B., & Chenna, D. K. (2020). Chemical reaction and radiation absorption effects on convective flows past a porous vertical wavy channel with traveling thermal waves. *International Journal of Fluid Mechanics Research, 47*(2), 153–169. https://doi.org/10.1615/InterJFluidMechRes.2020027296

[28] Sandeep, N., & Sulochana, C. (2018). Momentum and heat transfer behaviour of Jeffrey, Maxwell, and Oldroyd-B nanofluids past a stretching surface with non-uniform heat source/sink. *Ain Shams Engineering Journal, 9*(4), 517–524. https://doi.org/10.1016/j.asej.2016.02.008

[29] Abdela, Y., & Shanker, B. (2018). The influence of non-uniform heat source and thermal radiation on MHD stagnation point flow of Maxwell nanofluid over a linear stretching surface. *International Journal of Mathematics Trends and Technology, 56*(4), 271–288.

[30] Sajiol, S. (2019). Impact of non-uniform heat source/sink on magnetohydrodynamic Maxwell nanofluid flow over a convectively heated stretching surface with chemical reaction. *Journal of Nanofluids, 4*, 795–805.

[31] Hashmi, S. M., Al-Khaled, K., Khan, N., Khan, S. U., & Tlili, I. (2020). Buoyancy-driven mixed convection flow of magnetized Maxwell fluid with homogeneous–heterogeneous reaction and convective boundary condition. *Results in Physics, 19*, 103379.

[32] Islam, S., Khan, A., Kumar, P., Alrabaiah, H., Shah, Z., Khan, W., Zubair, M., & Jawad, M. (2020). Radiative mixed convection flow of Maxwell nanofluid over a stretching cylinder with Joule heating and heat source/sink effect. *Scientific Reports, 10*, 17823.

[33] Aliakbar, V., Pahlavan, A. A., & Sadeghy, A. (2009). The influence of thermal radiation on MHD flow of Maxwellian fluids above stretching sheets. *Communications in Nonlinear Science and Numerical Simulation, 14*, 779–794. https://doi.org/10.1016/j.cnsns.2007.12.003

[34] Stanford, S. (2013). A new numerical approach to MHD flow of Maxwell fluid past a vertical stretching sheet in the presence of thermophoresis and chemical reaction. *Boundary Value Problems, 2013*, 196.

[35] Shah, S., & Hussain, S. (2021). Slip effect on mixed convective flow and heat transfer of magnetized UCM fluid through a porous medium in consequence of a novel heat flux model. *Results in Physics, 20*, 103749.

[36] Sandeep, N., Shivakumara, U., Sulochana, C., & Ashwinkumar, G. P. (2025). Enhanced thermal conductivity of the Carreau nanoliquid using Maxwell/Xue nanomodels. *Numerical Heat Transfer, Part A: Applications, 86*(19), 6847–6864. https://doi.org/10.1080/10407782.2024.2345861

[37] Ashwinkumar, G. P., Ranjana, B., Sandeep, N., & Sulochana, C. (2025). Transpiration effects on magneto-flow of ternary hybrid nanofluid above an exponentially elongating sheet. *Numerical Heat Transfer, Part B: Fundamentals, 86*(10), 3432–3449. https://doi.org/10.1080/10407790.2024.2361127

[38] Sandeep, N., Ranjana, B., Sulochana, C., & Ashwinkumar, G. P. (2025). Significance of nanoparticle shape factors on MHD nanofluid flow across a slender surface. *International Journal of Modelling and Simulation, 45*(5), 1596–1612. https://doi.org/10.1080/02286203.2023.2296520

[39] Ashwinkumar, G. P. (2022). Micro and nanofluid convection with magnetic field effects for heat and mass transfer applications using MATLAB. In S. Pramanik (Ed.), *Recent advances in fluid dynamics* (pp. 75–90). CRC Press. https://doi.org/10.1201/9781003212874-5

[40] Sandeep, N., Nanda, P., & Ashwinkumar, G. P. (2022). Transpiration effect on Falkner–Skan bioconvective mixed nanoliquid flow above a poignant wedge. *Proceedings of the Institution of Mechanical Engineers, Part C: Journal of Mechanical Engineering Science, 237*(8). https://doi.org/10.1177/09544062221134387

[41] Kavita, J., Kalpana, S., Pooja, S., & Sharad, S. (2024). Effect of radiation and slip parameter on MHD mixed convective Casson fluid flow along a vertical stretching sheet. *Proceedings of the Institution of Mechanical Engineers, Part E: Journal of Process Mechanical Engineering, 239*(2), 627–644. https://doi.org/10.1177/0954408924123959